Bandwidth and group-velocity effects in nanosecond optical parametric amplifiers and oscillators

Arlee V. Smith

Department 1128, Sandia National Laboratories, Albuquerque, New Mexico 87185-1423

I numerically model broad-bandwidth optical parametric oscillation and amplification to explore the influence of pump bandwidth on conversion efficiency, injection seeding, and generated spectra. I also study narrow-bandwidth pumping of broad-bandwidth signal and idler waves. I show that the relative group velocities of the three waves have a critical effect on device performance in all cases and provide physical explanations for this. © 2005 Optical Society of America

OCIS codes: 190.4970, 190.2620, 190.4360, 190.4410.

1. INTRODUCTION

There are a number of interesting questions associated with broad spectral bandwidth in nanosecond optical parametric oscillators (OPOs) and amplifiers (OPAs). For example, there are conflicting claims in the literature and in OPO lore as to whether an OPO pumped by a broadband laser can produce a single-mode signal. Furthermore, in what will come as a surprise to many OPO users, White *et al.*[1–3] recently reported that even when pumped by a single-mode pump, a seeded OPO will in some cases fail to fully seed and instead generate a broadband signal. There are some surprising effects on conversion efficiency as well. Arisholm *et al.*[4] noted that, according to their model of unseeded OPOs pumped by single-mode lasers, when the group velocity (GV) of the pump differed sufficiently from those of the signal and idler, the OPO efficiency improved dramatically, accompanied by a large increase in the signal bandwidth. In this paper I explain how the relative GVs influence the efficiency and bandwidth of an OPO, as well as the ability to injection seed it. My physical arguments connect the observations of Arisholm *et al.*[4] with those of White *et al.*[3] I show that when an OPO is pumped by a single-mode pump, there can be a modulational instability of the signal wave that allows it to overcome the conversion limit imposed by backconversion, leading to simultaneous increases in efficiency and bandwidth and to the loss of injection seeding. Another important bandwidth issue is the effect of pump bandwidth on OPO and OPA conversion efficiency. It has long been claimed that if the pump bandwidth exceeds an acceptance bandwidth associated with the nonlinear crystal, the mixing efficiency will suffer. I show that this is sometimes true.

Numerical OPO and OPA models have been developed that account for both spatial and temporal structure of the three waves.[5–7] Such models are necessary if we wish to capture effects associated with coupling between the spatial and the temporal features of the beams. However, for the sake of speed we drop the spatial effects in this pa-

per and model only plane-wave interactions of three temporally structured waves. The literature contains descriptions of several plane-wave OPA and OPO models that include GV and group-velocity dispersion (GVD).[8,9] The studies presented here are based on such models but the bandwidths are narrow enough that we can neglect GVD. Even with these simplifications, modeling studies are time-consuming because the model must use a time grid that is fine enough to fully resolve the time structure of all the waves and also because results can in some cases vary substantially from pulse to pulse, reflecting the random nature of the multimode pump light or the random nature of the quantum noise that is parametrically amplified in broadband signal or idler waves. These numerical models are freely distributed,[10] so anyone can model the exact device that interests them or repeat the calculations presented here. The goal of this paper is to point out some qualitative trends that can provide physical insight and guidance in device design. To highlight these trends we use standard sets of mixing parameters whenever possible. Most of the parameters correspond to parametric amplification in a KTP crystal for the wavelengths (532 nm → 800 nm + 1588.1 nm), except we change the GVs and linewidths at will to explore various bandwidth effects.

With these models we use a conventional split-step method in which the computation of linear propagation and nonlinear mixing are alternated for each small propagation step. Propagation is computed using Fourier-transform methods, whereas mixing is handled by Runge–Kutta integration. Reference 9 presents a detailed description of the OPO model. Our standard OPO is a three-mirror ring comprising a left mirror, a right mirror, and a totally reflecting mirror. The crystal is located between the left and the right mirror, and the OPO is pumped through the left mirror with outputs through the right mirror. The parameters for this standard OPO are listed in Table 1 and those for our standard OPA are listed in Table 2. The plane-wave irradiances at the input to the

Table 1. Standard OPO Model Input Parameters

Parameter	Signal	Idler	Pump
Wavelength (nm)	800	1588.1	532
Refractive index	1.817	1.736	1.790
GV index	1.95	2.05	2.0–2.5
Pulse energy (mJ)		0	0–20
Power (W)	0–10^{-3}	0	
Beam diameter (mm)	1	1	1
Pulse duration (ns)	cw	cw	3
Left mirror reflectivity	0.99	0.99	0.00
Right mirror reflectivity	0.7	0–0.7	0.00
Linewidth (cm^{-1})			0–3
d_{eff} (pm/V)	3.2		
Cavity length (mm)	30		
Crystal length (mm)	10		
Δk (mm^{-1})	0		

devices are those corresponding to the center of Gaussian beams with the diameter, duration, and energy or power specified in Tables 1 and 2. For singly resonant OPOs, only the signal wave is recirculated. For doubly resonant OPOs, both the signal and the idler are recirculated but the pump is not. The OPO seed light, when present, is cw with a power of 1 mW incident on the right mirror, or output coupler, and it is always tuned to exact resonance with the cavity.

Unseeded OPAs and OPOs are initiated by the quantum optical backgrounds at the signal and idler frequencies. To model this we fill a set of longitudinal modes over a bandwidth several times greater than the crystal's acceptance bandwidth, spaced by ~100 MHz, with fields that have a Gaussian distribution of amplitudes and a random distribution of phases. This random noise is normalized to a level of one photon per mode as a classical approximation of the quantum background. It is transformed to the time domain, and the coherent seed light field, if present, is added to it. The OPO or OPA amplifies this random light and in the process imposes a spectrum on the amplified light determined primarily by the GVs of the three waves in the crystal and, in the case of an OPO, also by recirculation in the cavity. Similarly, the broad-bandwidth nanosecond lasers that are often used to pump OPOs and OPAs usually amplify a quantum background with a bandwidth determined by the linewidth of the gain medium. We simulate a broadband pump by filling a set of longitudinal modes with light with random phase and Gaussian amplitude distribution. A typical mode spacing is 250 MHz, and the number of modes is varied to accommodate different bandwidths. This field is transformed to the time domain, and a 3 ns Gaussian envelope is imposed. In the time domain the resulting pulse exhibits the strong mode beating familiar for broadband nanosecond lasers. In situations where the output fluences or spectra vary substantially from run to run due to the random variations of the seed or pump light, we typically repeat the model run five to ten times with different starting fields and average the results.

Previous reports have pointed out that including realistic spatial profiles, diffraction, and birefringence can re-

duce the effect of bandwidth effects, and it can introduce bandwidth-related effects that cannot be seen in plane-wave models.[6,7,9] The strength of the bandwidth effects presented here may be somewhat muted in laboratory devices due to averaging over spatial profiles. However, they should be evident at nearly full strength in waveguide devices or in devices with Fresnel numbers near unity. Examples include OPAs that use optimally focused collinear beams in noncritically phase-matched crystals or low-energy OPOs that are based on stable cavities that support only a single transverse mode.

It is no surprise that the relative GVs of the three interacting waves play a key role in the parametric process because they are directly related to the acceptance bandwidths. A common definition of the acceptance bandwidth for the signal and idler when the pump is monochromatic is given by the condition

$$|\Delta k L| \leq 2\pi, \tag{1}$$

where $\Delta k = k_p - k_s - k_i$ with p, s, and i standing for pump, signal, and idler; and L is the crystal length. For a fixed pump frequency, the signal and idler tune in opposite directions making $\Delta\omega_s = -\Delta\omega_i$; and we can expand Δk about the phase-matching point ($\Delta k = 0$) as

$$\Delta k = \left(\frac{dk_s}{d\omega_s} - \frac{dk_i}{d\omega_i}\right)\Delta\omega_i. \tag{2}$$

We write the GV defined by $v_g = d\omega/dk$ and as $v_g = c/n_g$ where n_g is the GV index, analogous to a refractive index. Equation (2) can be combined with inequality (1) to give

$$|\Delta k| = \left|\left(\frac{n_{g,s}}{c} - \frac{n_{g,i}}{c}\right)\Delta\omega_i\right| = \frac{2\pi}{L}, \tag{3}$$

so the relation between the GVs and the signal–idler acceptance bandwidth $\Delta\omega_{si}$ is

$$\Delta\omega_{si} = \left|\frac{2\pi c}{L(n_{g,s} - n_{g,i})}\right|. \tag{4}$$

The temporal walk-off between the signal and the idler waves in traversing the length of the crystal is $\tau_{si} = L(n_{g,s} - n_{g,i})/c$, making the signal–idler acceptance bandwidth $\Delta\nu_{si}$ the inverse of the signal–idler walk-off:

$$\Delta\nu_{si} = \Delta\omega_{si}/2\pi = |1/\tau_{si}|. \tag{5}$$

Table 2. Standard OPA Model Input Parameters

Parameter	Signal	Idler	Pump
Wavelength (nm)	800	1588.1	532
Refractive index	1.817	1.736	1.790
GV index	1.9–2.5	1.9–2.5	2–2.5
Pulse energy (mJ)	5×10^{-6}	0	1–150
Beam diameter (mm)	1		1
Pulse duration (ns)	3		3
Linewidth (cm^{-1})	0–4		0–4
d_{eff} (pm/V)	3.2		
Crystal length (mm)	10		
Δk (mm^{-1})	0		

The physical connection between walk-off and bandwidth is straightforward. In parametric gain the signal mixes with the pump to produce the idler wave; the idler wave in turn mixes with the pump to generate more signal wave. For a monochromatic pump and a single pass of the crystal this leads to a temporal correlation between the phases and the amplitudes of the signal and idler waves that extends over a time interval of τ_{si}. These correlations limit the spectral width of the signal and the idler to $\Delta\nu = 1/\tau_{si}$. In an OPO the signal (and the idler in doubly resonant OPOs) makes several passes of the crystal, and consequently the signal linewidth is often several times narrower than the acceptance bandwidth. However, we will show that this is not a general rule, and OPO and OPA linewidths can be broader than $\Delta\nu_{si}$, even when the pump is single mode.

We can define two additional acceptance bandwidths, based on the assumption that either the signal or the idler rather than the pump wave is single mode and the other two waves are spectrally broad. If the signal is single mode, the idler and pump waves tune together, and the acceptance bandwidth for this mixing process is

$$\Delta\nu_{pi} = |1/\tau_{pi}|, \qquad (6)$$

where τ_{pi} is the walk-off between pump and idler. Similarly, if the idler is single mode, the acceptance bandwidth for the signal and pump is

$$\Delta\nu_{ps} = |1/\tau_{ps}|. \qquad (7)$$

It has long been recognized that these two acceptance bandwidths also play important roles in broadband parametric amplification. For example, if a narrowband signal wave is amplified using a broadband pump, the broad pump on first entering the crystal will generate an idler wave that is locked in amplitude and phase to the pump and thus has the same spectrum. If the idler and pump have identical GVs, the phases of the idler and pump can continue to mimic one another, so no phase structure is added to the signal wave. On the other hand, if the pump and idler GVs differ, the idler wave can no longer carry away the phase variations of the pump. The spectral energy of the pump that lies outside the acceptance bandwidth $\Delta\nu_{pi} = 1/|\tau_{pi}|$ cannot fully contribute to the amplification of the idler unless it spectrally broadens the signal wave. As a consequence, when the pump wave has a phase structure on a time scale shorter than τ_{pi}, the signal–idler amplification will be reduced, and it will be accompanied by spectral broadening of the signal wave.

We have belabored this connection between acceptance bands and temporal walk-off as a reminder that a description of nonlinear mixing in terms of time-structured waves moving with different GVs is complete and fully accounts for acceptance bandwidths.

For later reference we define the quantities $\bar{n}_g$, $\bar{\tau}$, and Δ_p as

$$\bar{n}_g = (n_{g,s} + n_{g,i})/2, \qquad (8)$$

$$\bar{\tau} = L(n_{g,p} - \bar{n}_g)/c, \qquad (9)$$
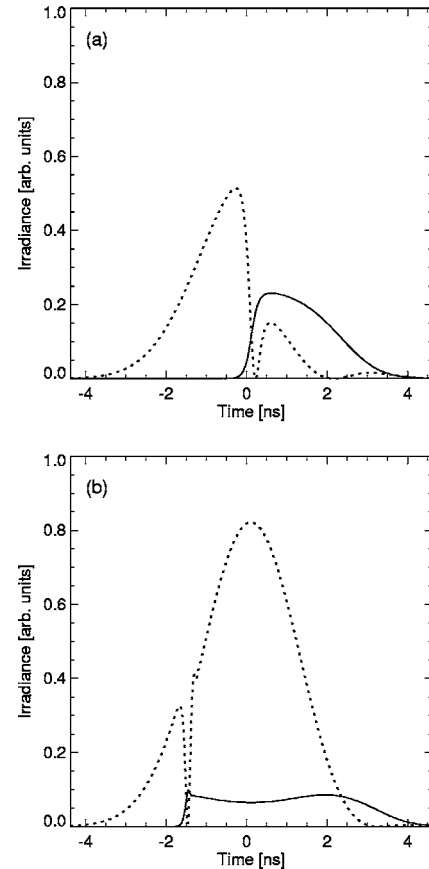
Fig. 1. Signal (solid curve) and transmitted pump (dotted curve) for a singly resonant OPO pumped by a single-mode laser (a) near threshold and (b) approximately five times threshold. The vertical scales in (a) and (b) are different.

$$\Delta_p = \frac{\bar{\tau}}{\tau_{si}} = \frac{n_{g,p} - \bar{n}_g}{n_{g,i} - n_{g,s}}. \qquad (10)$$

The value of $\bar{n}_g$ is 2.0 throughout this paper, and Δ_p is the walk-off of a pump pulse relative to a pulse whose GV is approximately midway between those of the signal and idler, normalized to the signal–idler walk-off. We will find that Δ_p is an important parameter in characterizing OPOs and OPAs pumped by a single-mode pulse.

2. MONOCHROMATIC PUMPING

This section is devoted to OPOs and OPAs pumped by single-mode pump pulses. Broadband pumping will be discussed in Section 3. To set the stage for our discussion of the effects of broadband signal and idler waves we first look at single-mode operation of a singly resonant OPO. For this reference case we force the model to treat all three waves as monochromatic. Figures 1(a) and 1(b) show typical signal and pump output pulses from the standard OPO operated near threshold and at approximately five times threshold, respectively. The important point is that, for pump levels approximately five times threshold and higher, the signal fluence strongly saturates due to backconversion. The reason is that the gain per pass must be high to turn the OPO on within the duration of the pump pulse; but after the OPO is turned on,

this high gain leads to reconversion of the signal and idler into pump light within one pass of the crystal. The resulting negative feedback to the signal amplitude tends to clamp the signal and idler at a rather constant and low level after turn on, as seen in Fig. 1(b). The signal fluence versus pump fluence for the reference case is shown in Fig. 2. The performance of the standard doubly resonant OPO is similar. The exact values of the signal and pump fluences differ, but the strong saturation due to backconversion is qualitatively the same.

A. Seeded Singly Resonant Optical Parametric Oscillator

We now remove the artificial restriction that the signal and idler waves must be monochromatic; otherwise the device is the same singly resonant OPO as before. Seeding the signal wave with 1 mW of cw light gives the performance shown in Fig. 3(a) for various pump GVs. When $n_{g,p}$ is midway between the signal and the idler GV indices ($\Delta_p = 0$), the performance is identical to the reference case of forced monochromatic waves. The efficiency is identical, and the signal is always single mode. In contrast, when $n_{g,p}$ is changed to 2.5 so that the pump travels significantly slower than the signal and idler ($\Delta_p = 5$), the efficiency follows the reference case only at low pump fluences. There is a breakpoint at a pump level approximately five times threshold above which the signal strength grows rapidly compared with the reference case, and this increased signal strength is correlated with a dramatic increase in the signal linewidth. Above the breakpoint, injection seeding partially fails, and the signal linewidth increases with increasing pump level to a maximum width of ~ 40 cm^{-1}, which is approximately four times $\Delta\nu_{\text{si}}$. The seeding failure is only partial in the sense that, early in the output signal pulse, injection seeding is effective and the signal and idler are monochromatic, but, part way through the pulse, additional frequencies appear in the signal and idler waves and remain strong for the remainder of the pulse. In the spectrum of the full pulse the seeded mode is strongest but the other modes collectively contain most of the signal energy. Figure 3(a) shows that for values of $n_{g,p}$ intermediate between 2.0 and 2.5 ($0 < \Delta_p < 5$) the breakpoint varies, with lower breakpoints associated with larger values of Δ_p.
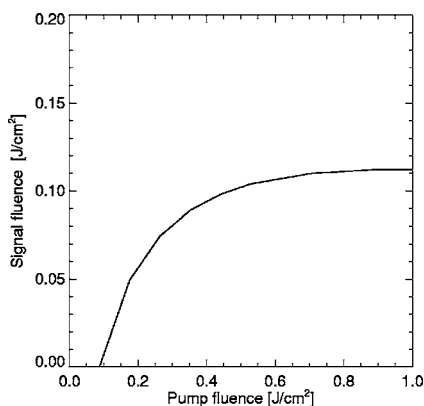
Fig. 2. Signal fluence versus input pump fluence for the standard, seeded, singly resonant OPO pumped by a single-mode pump.
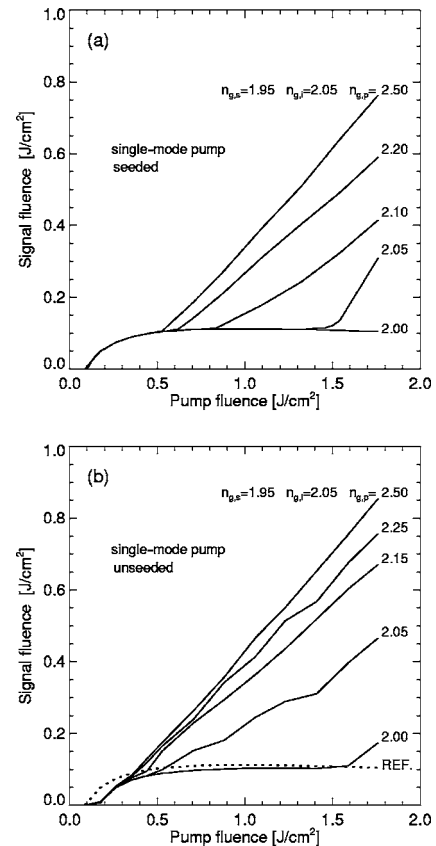
Fig. 3. Signal fluence versus pump fluence for the standard OPO with fixed signal and idler GVs ($n_{g,s} = 1.95$ and $n_{g,i} = 2.05$) but with varying values of the pump GV index $n_{g,p}$. (a) Seeded operation, (b) unseeded operation. Curves only for $n_{g,p} > 2$ are shown because those for $n_{g,p} < 2$ by the same amount are nearly identical.

Qualitatively, the behavior is similar for intermediate values of Δ_p. For pump levels above the breakpoint, the seeding partially fails, the spectrum broadens, and the efficiency improves.

It is tempting to explain the failure of injection seeding by noting that in the regime of strong backconversion the pump wave is only slightly depleted, so the unseeded modes could experience high gain and eventually overtake the seeded mode.[11] Although it is true that the pump is weakly depleted, it has a phase reversal approximately midway through the crystal; so if a particular unseeded signal mode is amplified in the first part of the crystal, it is deamplified in the later part and the net gain is suppressed, just as it is for the seeded mode. However, this is true only for small values of Δk, that is, for modes close in frequency to the seeded mode. If the modal frequency is offset so that $\Delta k L = \pi$, the mode can experience gain in both halves of the crystal because of the rephasing of the waves caused by their mismatched phase velocities. Indeed, for pump fluences that lie just above the breakpoint we find that modes detuned from the seeded mode by approximately $\Delta\nu_{\text{si}}/2$ are the only ones added to the signal spectrum.

However, this is an incomplete description of seeding failure. In the portion of the signal pulse after the appearance of the multiple unseeded modes, we find that the sig-
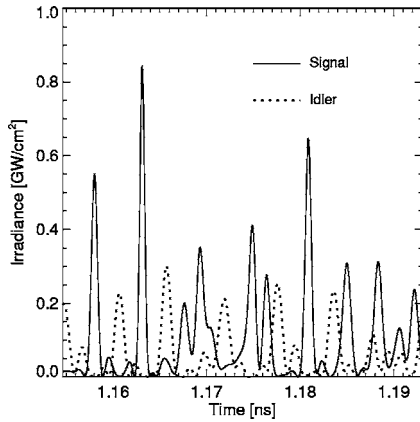
Fig. 4. Signal (solid curve) and idler (dotted curve) irradiance near the pulse center for ($n_{g,s}=1.95$, $n_{g,i}=2.05$, $n_{g,p}=2.5$) illustrating the pulsed nature of the signal and idler. The pump fluence is approximately 0.9 J/cm^2.

nal consists of a train of pulses, as shown in Fig. 4, rather than the random fluctuations that would be characteristic of independently oscillating modes. This implies that the modes are not amplified independently but rather their amplitudes and phases are coordinated in a way that leads to strong amplitude modulation at an appropriate modulation frequency. The coupling between signal modes is through their mutual modification of the pump wave. Because the signal and idler waves have a fairly well-organized structure in their time profiles, a description in terms of time modulation seems more likely to provide physical insight to analyze the departure from seeding than one in terms of spectral content alone.

If we accept the notion that the OPO prefers to maximize the energy stored in the resonated signal wave, operation in the realm of strong backconversion is unstable in the sense that it would be possible to store more energy if backconversion were defeated. Backconversion can be overcome if the signal evolves into a series of pulses with duration τ_{si} or less, rather than the unmodulated low-level characteristic of seeded operation. In a simplified description, idler pulses would be generated in synchrony with the signal pulses in the first part of the crystal but they would travel with a different GV, so the signal and idler pulses would lose overlap later in the crystal and this would weaken the backconversion. If the pump GV is midway between the signal and the idler velocities, only small portions of the pump would be depleted. However, if the pump GV is sufficiently different from those of the signal and idler, the pump energy slides past the signal and idler pulses and could be efficiently transferred to the signal and idler over the full time profile of the pump pulse. Efficient pump depletion requires the pump to walk off from the signal and idler by an amount at least equal to the signal pulse separation, which is approximately τ_{si}.

If this picture is correct, the duration of the signal and idler pulses should be approximately equal to the signal–idler walk-off τ_{si}. In our standard OPO, the value of τ_{si} is 3.3 ps. According to Fig. 4 the pulse separation of the signal and idler pulses predicted by the model is ~4.5 ps, in reasonable agreement. Furthermore, Fig. 4 shows that the output signal and idler pulses are generally offset in time so that backconversion is reduced. The walk-off of

the pump relative to the signal and idler is ~17 ps for $n_{g,p}=2.5$ ($\Delta_p=5$). This is much larger than the signal and idler pulse separations of 4.5 ps, so the pump can be effectively depleted. We expect the threshold for multimode operation, which we will call the unseeding threshold, to be lowest when the pump walk-off relative to the signal and idler is equal to or greater than the signal–idler walk-off, that is, when $\Delta_p>1$. Figure 5 shows a plot of the unseeding threshold versus Δ_p. Our conjecture appears valid. The unseeding threshold depends critically on the relative GVs. For a pump GV much different from the signal and idler velocities ($\Delta_p>1$), the unseeding threshold is approximately five times the seeded threshold; for a pump GV close to the signal and idler velocities ($\Delta_p<1$), the unseeding threshold is much higher. We have also used values of $n_{g,s}$ and $n_{g,i}$ different from the standard values of 1.95 and 2.05, and we find nearly identical curves for the unseeding threshold as a function of the normalized pump GV offset Δ_p. We do not expect identical curves for OPOs with other designs, but we expect this general pattern to apply.

The coupling between signal modes that is implied by the formation of pulse trains can be described as a modulational instability of the signal wave. Small amplitude variations in the nearly monochromatic early signal wave that have the proper spacing to avoid backconversion would be preferentially amplified until a train of pulses forms. If the pump walk-off is large compared with the pulse width, the gain remains high as these pulses develop because the pump is not more depleted near the peaks than elsewhere.

It is valid to question whether the breakdown of seeding predicted by our model is simply a numerical instability or quirk of the model rather than a genuine physical phenomenon. There is indeed some numerical noise in our model that is associated with splicing together sequential round-trip intervals of the signal field. However, I verified that this numerical noise is small compared with the noise introduced by the simulated quantum background. I believe that the results represent real physical effects rather than model artifacts. This conclusion is strongly supported by observations of seeding failure in an OPO reported recently by White et al.[1–3] White's OPO uses a 20 mm long, periodically poled crystal of KTP in a stable bowtie cavity of length 120 mm. It operates with a
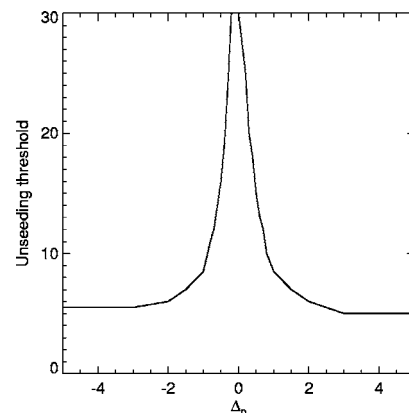
Fig. 5. Pump fluence at threshold of seeding failure, expressed in units of the seeded threshold, versus Δ_p.

Table 3. White's OPO Model Parameters

Parameter	Signal	Idler	Pump
Wavelength (nm)	840	1451	532
Refractive index	1.841	1.818	1.888
GV index	1.900	1.854	2.061
Pulse energy (mJ)		0	0–20
Power (W)	10^{-3}		
Beam diameter (mm)	1		1
Pulse duration (ns)	cw		25
Left mirror reflectivity	0.99	0.99	0
Right mirror reflectivity	0.64	0	0
d_{eff} (pm/V)	10		
Cavity length (mm)	120		
Crystal length (mm)	20		
Δk (mm^{-1})	0		

Fresnel number near unity, so it should be particularly amenable to modeling by our plane-wave model. Table 3 gives the full list of the model parameters used to simulate this OPO. As a first check we compare efficiency curves predicted by our model and measured by White *et al.* Figure 6 shows our results for seeded and unseeded operation. The dotted curve shows the performance for artificially forced monochromatic oscillation. The solid curve shows the simulated performance when the OPO is seeded, and the dashed curve shows the performance when it is unseeded. Qualitatively, the agreement between the computed efficiency plots shown in Fig. 6 and those in Fig. 3 of White *et al.*[2] is good. The slopes are different, perhaps due to our neglect of the transverse profile, but the ratio of the seeded and unseeded thresholds is accurate, and the crossing of seeded and unseeded curves at approximately four times threshold is in agreement. We note that the breakpoint where seeding fails in our simulation lies at approximately five times the seeded threshold, which is just above the upper limit of White's plot.

At a pump level of 0.088 J/cm^2, which is slightly above the breakpoint according to our model, the simulated signal and pump pulses are those shown in Fig. 7(a). Early in the pulse the signal is seeded, but at approximately the 5 ns point, other modes begin to oscillate. The traces in Fig. 7(a) are smoothed to simplify the display. The actual signal trace is nearly 100% amplitude modulated past the 5 ns point, as shown in Fig. 7(b) that displays unsmoothed traces for a short time slice near 10 ns. The signal and idler waves have evolved into trains of pulses with durations approximately equal to the signal–idler walk-off of 5.5 ps, and there is a time offset between the signal and the idler spikes. The value of Δ_p is 3.9, so the pump walk-off is approximately four times the signal–idler walk-off. This large pump walk-off permits the high level of pump depletion seen in Fig. 7(b).

Comparing our simulations with the time profiles for the signal and pump presented in Figs. 4 and 5 of Ref. 3, we find good qualitative agreement. They report that at a pump level five times the seeded threshold, seeding fails midway through the pulse, in agreement with our predictions. Another point of agreement is that when Δk

= 0.5 mm^{-1} instead of zero, the onset of seeding failure moves ~6 ns earlier in the pulse in both measurements and simulations. The only qualitative disagreement is that the failure of seeding appears to be less abrupt in the measurements than in the model.

We conclude that an instability of the signal wave that preferentially amplifies signal amplitude modulations of a certain duration can lead to seeding failure, particularly if the GV of the pump is quite different from the signal and idler velocities. More quantitatively, when $\Delta_p > 1$, seeding fails part way through the pulse if the OPO is pumped several times the threshold. For pump levels above the breakpoint in the efficiency curves, seeding fails, the efficiency improves, and the bandwidth broadens to several times $\Delta\nu_{si}$. This effect had not been reported until recently, perhaps because of the dual requirement of strong pumping and a large pump walk-off. This is a combination most likely encountered in quasi-phase-matched OPOs. Quasi-phase matching compensates for the phase velocity differences but does not compensate the GVs as birefringent phase matching tends to do, and this can lead to large values of Δ_p. In addition, quasi-phase-matched crystals are often relatively long and values for d_{eff} are large, so threshold fluences can be low, making it possible to pump an OPO at several times the threshold without encountering the optical damage limit.

B. Unseeded Singly Resonant Optical Parametric Oscillator

Many of the features noted above for the seeded OPO also apply to unseeded operation. Figure 3(b) shows efficiency curves for the standard OPO, again pumped by a single-mode laser, but without signal seeding. Compared with the seeded operation shown in Fig. 3(a), the threshold is higher, reflecting the fact that the signal and idler start from the quantum background rather than the much higher value of 1 mW in the seeded signal mode. When the pump GV index is midway between the signal and the idler indices ($\Delta_p = 0$), the efficiency remains slightly lower than the dotted reference curve even for pump levels many times the threshold. If we increase the value of Δ_p, the efficiency curves break away from the reference curve at progressively lower pump levels, typically only a few
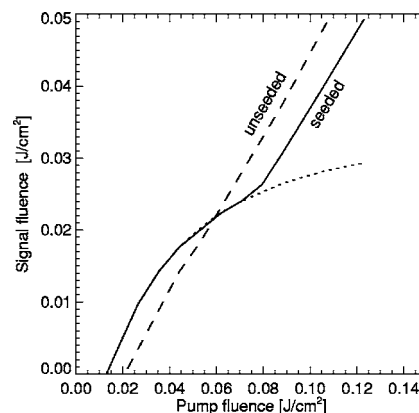
Fig. 6.   Signal fluence versus pump fluence for seeded and unseeded operation in simulations of the OPO of White *et al.* The dotted curve is the reference of Fig. 2 for forced monochromatic operation.
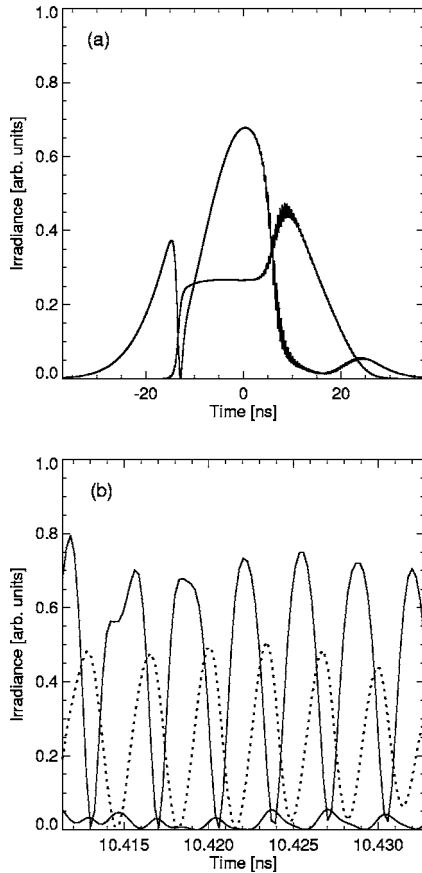
Fig. 7. (a) Simulation of White's seeded OPO at a pump fluence of 0.088 J/cm^2 (approximately five times threshold). Only the pump and signal traces are shown, and they have been smoothed to improve the display. The actual signal trace shows 100% modulation shortly after the breakdown of seeding as shown in (b) that displays a short time segment of the signal (upper solid curve), idler (dotted curve), and pump (lower solid curve) pulses without smoothing, near 10.4 ns. The vertical scales are identical in (a) and (b).

times the threshold, and the slopes of the efficiency curves above the breakpoint progressively increase. Increasing the pump level also increases the simulated signal linewidth from 2 to 4 cm^{-1} near threshold, which is 1/4–1/2 of $\Delta\nu_{si}$, to several times $\Delta\nu_{si}$, similar to the line-broadening trend seen in the seeded OPO.

Arisholm *et al.*[4] also modeled an unseeded OPO pumped by a single-mode pump in a study of the influence of GVs on backconversion, efficiency, and bandwidth. Their model was essentially the same as ours. They also found a striking variation in efficiency as the GV of the pump was varied relative to those of the closely spaced signal and idler velocities. Our observations match theirs.

Is the same instability that caused the signal wave to form a train of short pulses for seeded operation also responsible for the similar trends in efficiency and bandwidth in the unseeded OPO? Figure 8 shows short time slices of the simulated signal and idler waves for a pump level approximately five times the unseeded threshold. Figure 8(a) is for $n_{g,p}$ = 2.5 (Δ_p = 5), so the efficiency lies far above the reference curve according to Fig. 3(b); Fig. 8(b) is for $n_{g,p}$ = 2.0 (Δ_p = 0), so the efficiency lies near the reference curve. When Δ_p is large, as in Fig. 8(a), the signal

evolves into a series of pulses much as it did for the seeded OPO. In contrast, when Δ_p = 0 as in Fig. 8(b), the signal and idler waves are nearly constant in amplitude, and backconversion is just as strong as for the reference case of a monochromatic signal, even though the signal bandwidth is large. Amplitude modulation is suppressed, and the signal and idler are almost purely phase modulated. This is consistent with our earlier laboratory and model study of a nanosecond KTP OPO in which a strong tendency to generate phase-modulated signal waves was observed.[12,13] In that OPO the value of Δ_p was 0.8, and we pumped at levels less than four times threshold. We found that close to threshold the signal was broad and amplitude modulated, but as the pump was increased two to four times threshold, the signal became nearly purely phase modulated. This agreed well with simulations that we performed using the same OPO model used here. According to the model, at pump levels greater than four times threshold, the efficiency should increase and the phase modulation should be replaced by amplitude modulation. The linewidth should double from 2 to 4 cm^{-1}. The purity of the phase modulation in the laboratory device appeared to be more robust than in the model, but this might be because the Fresnel number of the laboratory OPO was large. The model predicts that, had we been able to pump the OPO at higher levels, we would have observed the reappearance of amplitude modulation accompanied by increases in efficiency and signal linewidth.
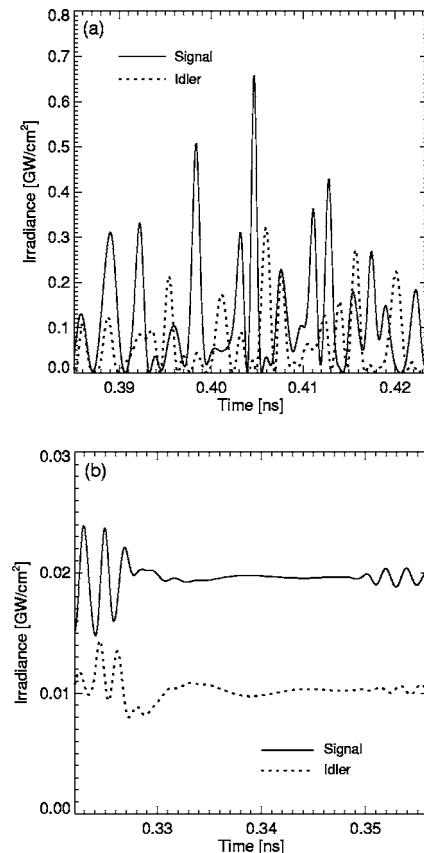
Fig. 8. Signal and idler irradiance near the center of the pump pulse for an unseeded OPO with a pump fluence of 0.9 J/cm^2 (approximately ten times threshold) with $n_{g,p}$ = (a) 2.5 and (b) 2.0.

There do not appear to be any definitive reports of laboratory observations of unseeded OPOs that support our predictions of unusually high efficiency accompanied by extra wide bandwidths when the pump is strong and $\Delta_p \neq 0$. That may be because the necessary pump levels are higher than the pump levels of one to five times threshold typical of many OPO experiments. In addition, real transverse beam profiles may tend to suppress this behavior to some extent.

C. Seeded Doubly Resonant Optical Parametric Oscillator

Many nanosecond OPOs are doubly resonant, either by design or by accident in cases where mirror transmission for the nominally unresonated wave is imperfect. How does double resonance affect efficiency and spectra? We look at the case of equal feedback of the signal and idler waves; in place of the 0.7 and 0.0 signal and idler feedback of the singly resonant OPO, we use 0.5 and 0.5 feedback. It is well known that the feedback phases of the signal (ϕ_s) and idler (ϕ_i) relative to the pump phase are important in a doubly resonant OPO. As our model is configured, if ($\phi_s + \phi_i = 0$), parametric gain is maximized; however, shifting ($\phi_s + \phi_i$) by π minimizes the gain. We model both cases. For the former, the OPO performs much like the singly resonant OPO. When the pump GV index is midway between those of the signal and idler ($\Delta_p = 0$), the OPO seeds well and the efficiency is low due to strong backconversion. When $\Delta_p \neq 0$, for example, $n_{g,p} = 2.5$ ($\Delta_p = 5$), seeding is effective at low pump levels, where the efficiency matches that for $\Delta_p = 0$; but at higher pump levels seeding fails, and the signal and idler are monochromatic early in the pulse but broadband late in the pulse. Seeding failure is accompanied by increased efficiency, just as in the singly resonant OPO.

We treat the low gain case by shifting the idler feedback phase by π while keeping the signal feedback phase fixed so the signal seed wave stays resonant with the OPO cavity. In this case seeding always fails. The threshold is several times higher, and the signal–idler spectra consist of clusters of modes positioned at $\pm\Delta\nu_{si}/2$ relative to phase matched and seeded frequency. The threshold is independent of Δ_p, but the efficiency slope increases with increasing pump walk-off. Thus at high pump levels the efficiency is minimum at $\Delta_p = 0$ and maximum at large values of Δ_p, just as it was for the doubly resonant OPO with feedback phases set for maximum gain.

D. Parametric Amplification

We next consider single-pass optical parametric amplification driven by a single-mode pump. The standard parameters are listed in Table 2. They are similar in most respects to the standard OPO parameters, with the primary difference being the much higher pump fluence that gives a much higher single-pass gain for the OPA. As a reference case we force all three waves to be monochromatic, and Fig. 9 shows the resulting pump depletion versus the pump fluence as the solid curve labeled Reference. Pump depletion initially rises steeply with pump fluence because of the high gain; but above the point where the pump is completely depleted at the peak of the pulse (pump fluence of ≈ 7 J/cm^2 in Fig. 9), backconversion re-
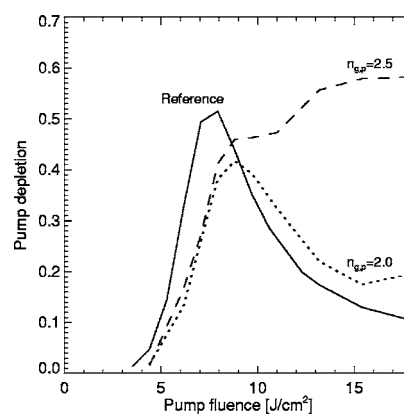
Fig. 9. Pump depletion for OPA with monochromatic pump and broad-bandwidth signal seed. The Reference curve is for all monochromatic waves. The lower curve is for $n_{g,s} = 1.9$, $n_{g,i} = 2.1$, and $n_{g,p} = 2.0$ and the upper curve is for $n_{g,s} = 1.9$, $n_{g,i} = 2.1$, and $n_{g,p} = 2.5$.

constitutes the pump from the signal and idler near the pulse center, reducing the net pump depletion. This raises the question of whether the suppression of conversion efficiency due to backconversion can be overcome by broadband signal–idler waves when $\Delta_p > 1$ as it was in the OPO.

To test this we amplify single-mode and broadband signal pulses using a monochromatic pump pulse. There is no idler input. When the input signal pulse is single mode, the output is also single mode, even for large values of Δ_p, and backconversion limits the conversion. We synthesize a multimode input signal pulse by choosing a modal frequency separation and a bandwidth and populate the modes with random phases and a Gaussian amplitude distribution. This is transformed to time, and a 3 ns Gaussian envelope is imposed. Typically we use a mode spacing of 0.1 cm^{-1} and a variable linewidth in the range of 0–4 cm^{-1}. We fix the signal and idler GVs at $n_{g,s} = 1.9$ and $n_{g,i} = 2.1$ and use two values for the pump GV, $n_{g,p} = 2.0$ ($\Delta_p = 0$) and $n_{g,p} = 2.5$ ($\Delta_p = 2.5$). Figure 9 shows the corresponding pump depletion as dotted and dashed curves. Clearly the effect of bandwidth is similar to that for an OPO. Backconversion is largely avoided when the pump walks off from the signal and idler ($n_{g,p} = 2.5$), but not when its GV index lies midway between those of the signal and idler ($giv_p = 2.0$).

If we fix the pump fluence at the strongly saturating value of 13 J/cm^2 and vary Δ_p, we obtain the curve shown in Fig. 10. The qualitative behavior of the OPA is similar to the OPO. Efficiency is lowest when $\Delta_p = 0$ and the width of the dip is approximately unity. Another similarity to OPOs is that when $|\Delta_p| > 1$ the linewidth of the signal and idler broaden to values several times ν_{si}.

3. BROADBAND PUMPING

Up to this point the pump pulse has always been single mode. In this section we study all of the devices discussed above, but using multimode rather than single-mode pump pulses. In our analyses in Section 2 we had two time scales to consider, the signal–idler walk-off time τ_{si} and the pump walk-off time relative to the signal–idler
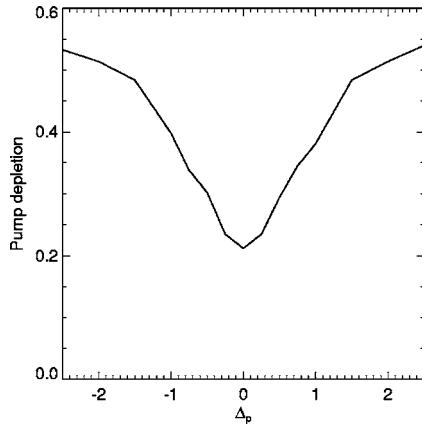
Fig. 10. OPA pump depletion versus the normalized temporal walk-off of the pump for a pump fluence of 13 J/cm^2. The pump is monochromatic; the signal and idler are broadband.

combination $\bar{\tau}$. The influence of these velocities became important only for strong pumping. Now we are adding a third time scale, the coherence time of the pump τ_{coh}. We will see that this added time scale can strongly affect OPO performance at low pump levels and that it is also important at all pump levels in OPAs. The questions of interest for broadband pumping are, under what circumstances can an OPO be seeded, how pure is the seeded spectrum, how does the pump bandwidth affect the conversion efficiency, and what is the influence of the GVs?

We argued above that if the pump and idler waves have identical GVs in a seeded OPO or OPA, the idler could mimic, or carry away, the phase variations of the pump, leaving the signal wave spectrally pure. On the other hand, if the pump and idler GVs are different enough that the walk-off between them is larger than the finest time structure of the pump ($\tau_{pi} > \tau_{coh}$), the idler cannot effectively counteract the pump phase. Consequently the signal phase will be modified by the amplification process. Another way of saying this is that, if the pump bandwidth is larger than $\Delta\nu_{ip}$ we expect the amplified signal wave to be phase modulated, and perhaps the OPO would seed poorly. We can also expect the small signal gain to be reduced because at the input end of the crystal the idler is generated with the phase that maximizes gain, but as the waves propagate with different GVs their relative phases deviate from the gain-maximizing value reducing the net gain, an effect we will call walk-off dephasing.

The argument for idler compensation of the pump phase is fully relevant only for a purely phase-modulated pump. In reality most multimode pump lasers generate light that is amplitude modulated as well as phase modulated. The amplitude modulation is transferred to the signal and idler waves leaving them with amplitude modulation on the time scale τ_{coh} or shorter. In the absence of gain, the signal and idler amplitude peaks would travel at their natural GVs, but high parametric gain tends to keep their amplitude spikes traveling together at a common velocity because of their mutual reinforcement. The effective velocity of the signal and idler structure at high gain lies somewhere between the signal and the idler velocities, and we can expect the difference between $n_{g,p}$ and $\bar{n}_g$ to once again play an important role in OPO and OPA performance.

A. Singly Resonant Optical Parametric Oscillator

1. Linewidth Pump of 0.3 cm^{-1}

For our study of seeded, singly resonant OPOs pumped by multimode pulses we use two different pump linewidths, one narrow enough that pump walk-off is insignificant compared with the pump coherence time ($\tau_{coh} > \bar{\tau}$), the other broad enough that it is significant ($\tau_{coh} < \bar{\tau}$). The OPO is seeded, and we keep the same signal and idler GVs as before ($n_{g,s}=1.95$, $n_{g,i}=2.05$), once again varying $n_{g,p}$ from 2.0 to 2.5. The first set of simulations uses a pump linewidth of 0.3 cm^{-1}, which is typical of many multimode Nd:YAG lasers. The pump coherence time is 110 ps, which is much larger than any of the walk-off times, so the primary effect of pump linewidth on the signal wave is through the pump wave's amplitude modulation that is impressed on the signal wave to some extent. The idler takes up the pump's phase modulation and hence has the same linewidth as the pump. Otherwise we might expect the performance to resemble the seeded OPO pumped by a single-mode pulse. Figure 11(a) displays results for pump fluences up to 20 times threshold. Note that the reference curve is the one computed above and represents OPO performance when all three waves are monochromatic. The efficiency curves of Fig. 11(a) should be compared with the corresponding results for a monochromatic pump shown in Fig. 3(a). The OPO performs nearly the same as with the single-mode pump, the notable exception being that the breakpoints in the effi-
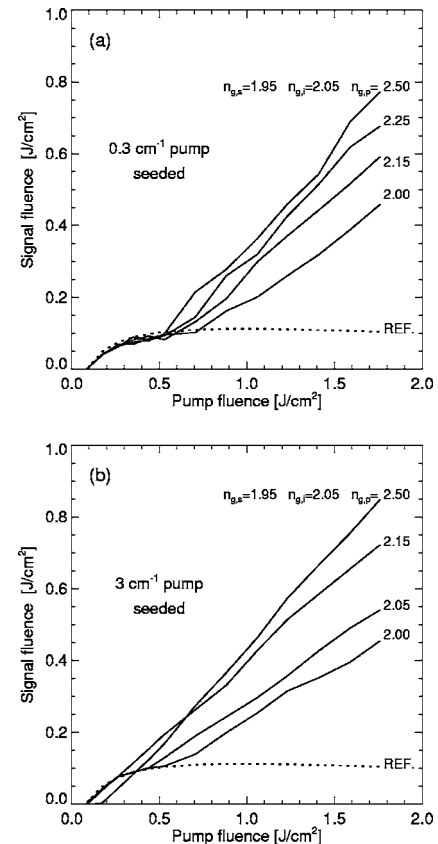
Fig. 11. Signal fluence versus pump fluence for (a) 0.3 cm^{-1} bandwidth pump and (b) a 3.0 cm^{-1} bandwidth pump. A signal seed is applied in all cases, but seeding is only partially successful.

ciency curves all lie at approximately five times threshold rather than depending strongly on $n_{g,p}$ as they did for the single-mode pump. The qualitative behavior above the breakpoint is also similar; early in the pulse the signal is seeded and narrowband, but later in the pulse it develops frequency sidebands and strong amplitude and phase modulation. When seeding fails, the amplitude spikes in the signal wave that we noted with monochromatic pumping are again in evidence. Another similarity is that the spectral width of the signal increases with increasing pump fluence, reaching widths several times $\Delta \nu_{si}$ at the highest pump levels. The lower breakpoints for multi-mode pumping compared with the single-mode pump are a consequence of the amplitude modulation impressed on the signal wave by the broadband pump. This modulation moves energy to the spectral wings, allowing the extra modes to grow starting from much higher levels than the quantum background level that applies for a monochromatic pump.

As Fig. 11(a) shows, from threshold to approximately five times threshold the efficiency is nearly identical to the reference case. In this region the signal wave is nearly single mode. Because of the amplitude modulation impressed on the signal by the amplitude variations of the pump, the signal has weak frequency sidebands, but each typically has less than 1% of the energy of the seeded mode. As a point of comparison with laboratory observations, He and Orr[14] reported single-mode performance of a singly resonant OPO seeded at 1550 nm and pumped by 1064 nm light from a multimode Nd:YAG laser. Their crystal was 19 mm long periodically poled lithium niobate (PPLN) for which the GVs of the 1064 nm pump and the 3390 nm idler are identical, $n_{g,p}=n_{g,i}=2.211$, whereas $n_{g,s}=2.182$. Because the pump walk-off of $\bar{\tau}=0.5$ ps is much less than its coherence time of $\tau_{coh} \approx 100$ ps, at low pump levels the signal should be amplitude modulated with little phase modulation. He and Orr used pump levels only up to twice threshold, limited by optical damage of the PPLN crystal, and they reported successful seeding throughout this range. Our simulations are compatible with this but imply that at higher pump levels the seeding will fail. He and Orr's measurement of the spectral purity of the signal indicates that the strength of spectral sidebands is <1% of the seeded mode, which is the approximate level of the sidebands in our simulations. They also report the range of Δk over which seeding is successful is ten times smaller for the multimode pump than for a single-mode pump. We find a similar effect in our simulation, except the range reduction is only a factor of 2 rather than 10.

The one exception to this similarity between model predictions for the 0.3 cm⁻¹ and monochromatic pumps at high pump levels is when $n_{g,p}=2.0$ ($\bar{\tau}=0$), in which case the efficiency for the multimode pump deviates from the reference curve. However, the increased efficiency above the breakpoint is not accompanied by spectral broadening of the signal for this particular GV. Seeding remains quite good up to the highest pump levels shown.

2. Linewidth Pump of 3.0 cm⁻¹

In Fig. 11(b) we show efficiency curves for the broader 3.0 cm⁻¹ linewidth pump that has a coherence time of 11
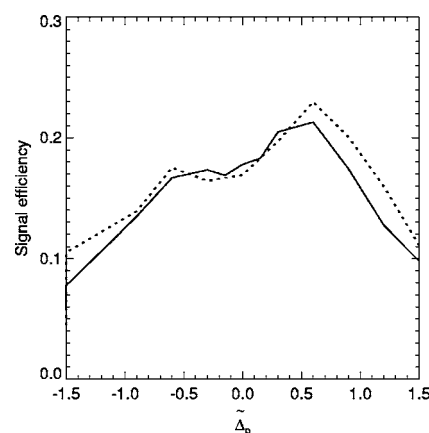
Fig. 12.   Signal efficiency versus pump walk-off for a singly resonant OPO pumped near threshold by a pump with a linewidth of 3 cm⁻¹. The solid curve is for $n_{g,s}=1.95$, $n_{g,i}=2.05$; the dotted curve is for $n_{g,s}=1.9$, $n_{g,i}=2.1$. $\tilde{\Delta}_p=(\bar{\tau}/\tau_{coh})$.

ps. At high pump levels the efficiency is high for all values of the pump walk-off. At pump levels below 0.5 J/cm² the efficiency follows the reference curve for small values of $\bar{\tau}$ and seeding is effective; but when $\bar{\tau}$ approaches τ_{coh} ($n_{g,p} > 2.15$), seeding fails entirely and the efficiency falls below the reference curve. Many nanosecond OPOs are operated within a factor of 5 of threshold, so it is worth examining this pump range in more detail. We fix the pump fluence at 0.35 J/cm² and calculate the signal efficiency (signal output fluence divided by pump input fluence) without seeding as a function of the pump GV. The results are shown in Fig. 12 for two cases: $n_{g,s}=1.95$, $n_{g,i}=2.05$ (solid curve) and $n_{g,s}=1.9$, $n_{g,i}=2.1$ (dotted curve). The horizontal scale is $\tilde{\Delta}_p=(\bar{\tau}/\tau_{coh})$, which is the pump walk-off normalized to the 11 ps coherence time of the pump. This normalization to τ_{coh} is to be contrasted with the normalization to τ_{si} that we showed to be relevant at high pump levels for both single-mode and multimode pumps. At this low pump level depletion of the pump is of secondary importance to the small signal gain when we are determining the efficiency, and the small signal gain is reduced by walk-off dephasing if the pump walk-off is larger than the pump coherence time ($|\tilde{\Delta}_p|<1$). When $n_{g,p}$ lies between the signal and the idler n_g's ($|\tilde{\Delta}_p|<0.5$), the signal spectrum narrows to 2 cm⁻¹, which is smaller than the values for $\Delta \nu_{si}$ of 5 and 10 cm⁻¹ for the two curves. When $n_{g,p}$ falls outside this range, the signal linewidth is approximately equal to $\Delta \nu_{si}$. Efficiency curves with seeding are similar, but seeding is successful only when $n_{g,p}=n_{g,i}$.

3. Varied Pump Linewidth

In Fig. 13 we take a different look at OPO efficiency near threshold. We keep the pump velocity fixed at $n_{g,p}=2.5$ and vary the pump bandwidth from 0 to 3 cm⁻¹. We show the performance with and without an applied signal seed in Figs. 13(a) and 13(b). For this large value of pump walk-off, seeding the signal fails in all cases except for a nearly monochromatic pump (the curve labeled 0 cm⁻¹), and this failure to seed is reflected in the shapes of the curves. As always, when seeding fails there is no back conversion and no saturation of signal fluence. A comparison of Figs. 13(a) and 13(b) shows that the threshold is
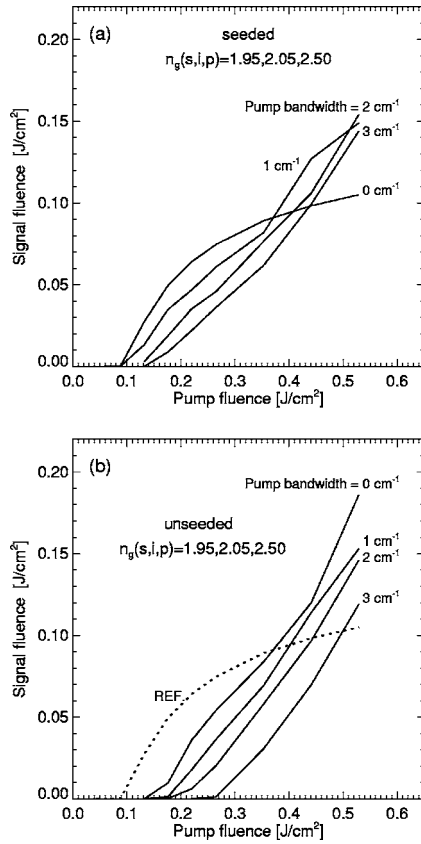
Fig. 13.   Signal fluence versus pump fluence for singly resonant OPO pumped by light with different bandwidths. (a) Signal seed, (b) unseeded. The dotted curve is the reference curve for seeded operation with monochromatic pumping; the solid curves are for pump bandwidths of 0, 1, 2, and 3 cm^{-1}. The GVs are indicated in the figure.

always higher when no seed is supplied, reflecting the lower starting value of the signal field. Furthermore, thresholds increase with pump bandwidth. We also note that the signal bandwidth increases with the pumping level in every case, from 1.5 to 3 cm^{-1} near threshold to 10–15 cm^{-1} at the highest pump level of 0.5 J/cm^2.

The increase in threshold and the reduction in efficiency with increasing pump bandwidths can be attributed to walk-off dephasing, which is important in the low gain regime. Over the first part of the crystal the signal and idler are amplified but later in the crystal, past the point where the phases shift by approximately π, they are deamplified. The broader the pump, the shorter the gain length and the lower the net gain.

B. Doubly Resonant Optical Parametric Oscillator
We pointed out above the importance of signal and idler feedback phases in the doubly resonant, monochromatically pumped OPO. In contrast, when the pump is broadband the feedback phases of the signal and idler are irrelevant because the phase of the pump is uncorrelated from one cavity pass to the next, unless the round-trip time of the pump source matches that of the OPO, a case that was studied by Arisholm et al.[15] In discussing singly resonant OPOs we pointed out that if the pump and idler GVs were similar, the idler phase could mimic the pump phase, making seeding of the signal easier. We antici-

pate that if this broadband idler is recirculated in the cavity along with the signal, even if $n_{g,p} = n_{g,i}$, the signal phase cannot remain constant and seeding will suffer. To illustrate this we used a signal feedback of 0.6 and an idler feedback of 0–0.1 in place of the standard OPO signal and idler feedback of 0.7 and 0.0. As a rule of thumb, we find that if the singly resonant OPO is operated under conditions that seed well with a broadband pump, adding 1% idler feedback will cause the signal to acquire sidebands with an amplitude of ~1% relative to the seeded mode, and the frequency spread of the sidebands will be equal to the pump bandwidth. If the signal and idler feedback are nearly equal, seeding the OPO fails entirely.

C. Parametric Amplification
Our final topic is OPA with a multimode pump and single-mode signal input. Compared with the OPO, the single-pass gain is much higher. We find that, in the strong pump regime where backconversion is important, the time scale that characterizes the structure of the signal and idler waves is the shorter of τ_{coh} and τ_{si}. This is different from narrowband pumping where τ_{si} was the characteristic time scale.

Figure 14 shows the same reference curve of pump depletion that we showed in Fig. 9 for OPA with three monochromatic waves. Figure 14 also shows pump depletion for a multimode pump with a single-mode input signal when all three n_g's are set equal (labeled AM). The change in shape compared with the reference curve is due only to the amplitude modulation of the pump because there is no temporal walk-off to change the relative phases of the waves. At low pump levels the depletion is higher than for the reference case because the amplitude modulation of the pump packs the pump energy into amplitude spikes that produce high gains over short time periods. As the pump level is increased, backconversion begins to limit the pump depletion and the AM curve rolls over at lower pump fluences than the reference curve. At the highest pump levels the AM and reference curves gradually merge. The AM curve can be regarded as a ref-
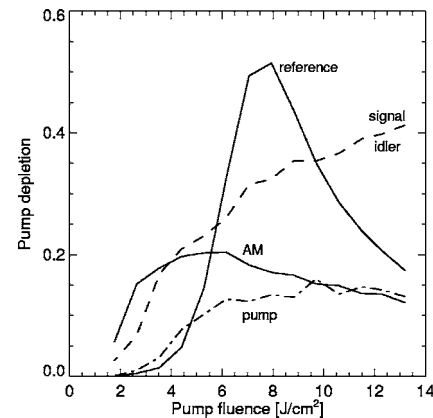
Fig. 14.   Pump depletion versus pump fluence for optical parametric amplification with a multimode pump pulse and single-mode signal seed. The curve labeled reference is for a single-mode pump; the curve labeled AM is for a multimode pump with all the GVs equal; the curves labeled signal, idler, and pump are for GV walk-off of one of the indicated waves relative to the other two. The temporal walk-off is 17 ps and the pump coherence time is 8.3 ps.
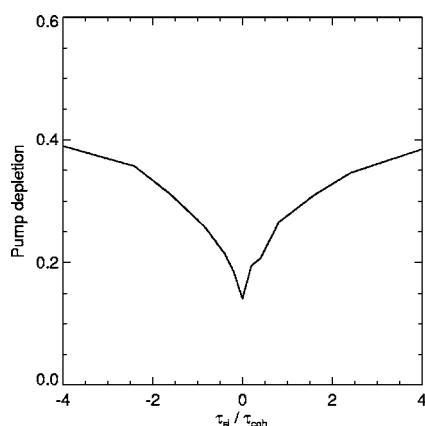
Fig. 15. Pump depletion in parametric amplification by a multimode pump versus the signal–idler walk-off (τ_{si}) normalized to the characteristic time of the pump variations $\tau_{coh}=8.3$ ps. The pump fluence is 8.8 J/cm^2.

erence curve for multimode pumps. In fact, when the three waves have equal GVs there is no difference between the pump depletion curves for pump bandwidths spanning the range we modeled, 0.3–4.0 cm^{-1}. The signal spectrum associated with the AM curve at low pump levels consists of one strong mode accompanied by low-level, amplitude-modulation-induced sidebands spread over a frequency range approximately equal to the pump bandwidth. Most of the signal energy resides in the sidebands, but the seeded frequency is the strongest individual frequency. At high pump levels multiple cycles of backconversion shorten the signal and idler amplitude spikes and also add phase reversals to the signal. This broadens the signal spectrum beyond that of the pump, but there is still one strong mode accompanied by many low-level sidebands.

The influence of adding GV differences between the waves is indicated by the two curves labeled pump and signal–idler. In both cases two of the waves are assigned equal velocities while the other walks off by 17 ps. The pump linewidth is 4 cm^{-1}, corresponding to $\tau_{coh}=8$ ps. The pump curve is for pump walk-off and deviates from the AM curve at low pump levels where walk-off dephasing is important. The signal–idler curve is for walk-off of either the signal or the idler and deviates from the AM curve at high pump levels where backconversion is important. As the signal–idler curve shows, if the signal and idler walk off from one another, the backconversion is largely defeated and efficiency is relatively high. The critical time scale is set by the typical duration of the pump variations τ_{coh}. The signal and idler develop structure early in the crystal with this time scale, and if the signal–idler walk-off time τ_{si} is comparable, backconversion can be avoided because of the poor temporal overlap of the signal and idler pulses. As a demonstration of this, Fig. 15 shows the pump depletion at an intermediate pump level of 8.8 J/cm^2 as τ_{si} is varied. The horizontal scale is τ_{si}/τ_{coh}, where in this case $\tau_{coh}=8$ ps.

All the multimode-pumped OPA cases described above were based on a single-mode signal seed. If we use a multimode signal seed with a bandwidth comparable to or less than the acceptance bandwidths, the efficiencies are slightly reduced. The study described above was also for

rather high parametric gain where the input signal energy of 5 nJ was amplified enough to deplete a pump of several millijoules. This implies gains of 10^6 or more at the highest pump fluences. We repeated the modeling using stronger 50 μJ signal pulses and lower gains and found that the details of the pump depletion curves change, but the trends and relative efficiencies are much the same. Taken together, these observations imply that the efficiency trends outlined here should also be expected in optical parametric generation driven by a multimode pump laser.

4. CONCLUSIONS

We simulated the operation of OPOs and OPAs pumped by single-mode and multimode pulses looking for trends that can serve as a guide in designing such devices, or at least can serve as a warning about conditions that might lead to undesired behavior. In the case of a single-mode pump we showed that at pump levels within a few times oscillation threshold, seeding is usually possible; but at higher pump levels the seeded state may be unstable to amplitude modulation of the signal and idler, and seeding may partially fail, meaning that the signal is seeded early in the pulse but not late. The onset of this instability depends strongly on the GV of the pump relative to those of the signal and idler. When seeding fails, conversion efficiency improves and signal–idler linewidths increase with increasing pump levels. Single-mode pumping of parametric amplification produces similar behavior. When the pump GV is close to the mean velocity of the signal and idler, backconversion suppresses efficiency at high pump levels; but when the pump GV differs from the mean by a large amount, the backconversion is defeated and efficiency rises along with the signal linewidth.

If the pump light is broadband, but with a coherence time long compared with any of the GV walk-off times, the qualitative behavior is similar to monochromatic pumping. Seeding the OPO is possible at low pump levels but not at high levels. However, if the pump coherence time is shorter than the walk-off times, seeding is impossible except when the pump GV is very close to the mean velocity of the signal and idler. At low pump levels the efficiency of a broadband-pumped OPO is highest when the pump velocity is close to the signal–idler mean and falls when the pump walk-off is larger than the pump coherence time. OPA efficiency is also sensitive to walk-off between the signal and idler waves at high pump levels.

Finally we mention that if the Fresnel number of an OPO or OPA is large, there may be a spatial analog of the effects we have studied, in which spatial structure and Poynting vector walk-off assume the roles of temporal structure and GV walk-off. This might allow the evolution of a lateral modulation of the signal wave to overcome backconversion, and this would be associated with poor beam quality and a large angular spectrum. Changing the angle of the pump beam in a noncollinearly pumped OPO could be used to vary the pump walk-off. Of course combinations of spatial and temporal structure are also possible. The understanding of such effects will require careful characterizations of devices with large Fresnel numbers. Modeling such effects requires the inclusion of

both spatial and temporal structure and spatial and temporal walk-off.[6] We hope that the results presented here will also serve as a starting point for such studies.

ACKNOWLEDGMENTS

REFERENCES AND NOTES

1. R. T. White, Y. He, B. J. Orr, M. Kono, and K. G. H. Baldwin, "Control of frequency chirp in nanosecond-pulsed laser spectroscopy. 1. Optical-heterodyne chirp analysis techniques," J. Opt. Soc. Am. B **21**, 1577–1585 (2004).
2. R. T. White, Y. He, B. J. Orr, M. Kono, and K. G. H. Baldwin, "Control of frequency chirp in nanosecond-pulsed laser spectroscopy. 2. A long-pulse optical parametric oscillator for narrow optical bandwidth," J. Opt. Soc. Am. B **21**, 1586–1594 (2004).
3. R. T. White, Y. He, B. J. Orr, M. Kono, and K. G. H. Baldwin, "Transition from single-mode to multimode operation of an injection-seeded pulsed optical parametric oscillator," Opt. Express **12**, 5655–5660 (2004).
4. G. Arisholm, G. Rustad, and K. Stenersen, "Importance of pump-beam group velocity for backconversion in optical parametric oscillators," J. Opt. Soc. Am. B **18**, 1882–1890 (2001).
5. G. Arisholm, "Quantum noise initiation and macroscopic fluctuations in optical parametric oscillators," J. Opt. Soc. Am. B **16**, 117–127 (1999).
6. A. V. Smith, D. J. Armstrong, M. C. Phillips, R. J. Gehr, and G. Arisholm, "Degenerate type I nanosecond optical parametric oscillators," J. Opt. Soc. Am. B **20**, 2319–2328 (2003).
7. W. J. Alford, R. J. Gehr, R. L. Schmitt, A. V. Smith, and G. Arisholm, "Beam tilt and angular dispersion in broad-bandwidth, nanosecond optical parametric oscillators," J. Opt. Soc. Am. B **16**, 1525–1532 (1999).
8. W. J. Alford and A. V. Smith, "Frequency-doubling broadband light in multiple crystals," J. Opt. Soc. Am. B **18**, 515–523 (2001).
9. A. V. Smith, R. J. Gehr, and M. S. Bowers, "Numerical models of broad-bandwidth nanosecond optical parametric oscillators," J. Opt. Soc. Am. B **16**, 609–619 (1999).
10. The OPO modeling uses SNLO function PW-OPO-BB and the OPA modeling uses SNLO function PW-mix-BB. SNLO is a public domain software available as a free download at http://www.sandia.gov/imrl/X1118/xxtal.htm.
11. E. S. Cassedy and M. Jain, "A theoretical study of injection tuning of optical parametric oscillators," IEEE J. Quantum Electron. **QE-15**, 1290–1301 (1979).
12. D. J. Armstrong and A. V. Smith, "Demonstration of a frequency-modulated, pulsed optical parametric oscillator," Appl. Phys. Lett. **70**, 1227–1229 (1997).
13. D. J. Armstrong and A. V. Smith, "Tendency of nanosecond optical parametric oscillators to produce purely phase-modulated light," Opt. Lett. **21**, 1634–1636 (1996).
14. Y. He and B. J. Orr, "Tunable single-mode operation of a pulsed optical parametric oscillator pumped by a multimode laser," Appl. Opt. **40**, 4836–4848 (2001).
15. G. Arisholm, E. Lippert, G. Rustad, and K. Stenersen, "Effect of resonator length on doubly resonant optical parametric oscillator pumped by a multilongitudinal-mode beam," Opt. Lett. **25**, 1654–1656 (2000).